Active noise control at a moving virtual microphone using the SOTDF moving virtual sensing method

Danielle J. Moreau, Ben S. Cazzolato and Anthony C. Zander

School of Mechanical Engineering, The University of Adelaide, Adelaide SA 5005 Australia

ABSTRACT

Traditional local active noise control systems minimise the measured acoustic sound pressure to generate a zone of quiet at a physical error sensor. The resulting zone of quiet is generally limited in size and as such, placement of a physical error sensor at the location of desired attenuation is required, which is often inconvenient. Virtual acoustic sensors can be used to project the zone of quiet away from a physical error sensor to a remote location. A number of virtual sensing algorithms have been developed in the past and these have shown potential to improve the performance of local active noise control systems. However, it is likely that the desired location of maximum attenuation is not spatially fixed. In this paper, a stochastically optimal virtual microphone capable of tracking a desired virtual location in a modally dense three-dimensional sound field is developed using the Stochastically Optimal Tonal Diffuse Field (SOTDF) moving virtual sensing method. The performance of an active noise control system in generating a zone of quiet at the ear of a rotating artificial head with the SOTDF moving virtual sensing method has been experimentally investigated and experimental results are presented here.

INTRODUCTION

Traditionally, passive techniques such as enclosures barriers and silencers have been used to minimise unwanted disturbances. While these devices do generate high attenuation over a broad frequency range, they are less effective at low frequencies and are relatively large in terms of size and cost (Hansen and Snyder 1997). Active noise control provides an alternative to passive techniques and has shown potential in minimising low frequency acoustic disturbances. Active noise control involves the use of secondary sound sources to cancel the primary noise disturbance, based on the principle of superposition, in which antinoise of equal amplitude but opposite phase is combined with the primary noise to cancel both disturbances (Hansen and Snyder 1997).

A local active noise control system creates a localised zone of quiet at the error sensor by minimising the acoustic pressure measured at the error sensor location with a secondary sound source. While significant attenuation may be achieved at the error sensor location, the zone of quiet is generally impractically small. Elliott et al. (1988) demonstrated both analytically and experimentally that the zone of quiet generated at a microphone in a pure tone diffuse sound field is defined by a *sinc* function, with the primary sound pressure level reduced by 10 dB over a sphere of diameter one tenth of the excitation wavelength, $\lambda/10$. As the zone of quiet generated at the error sensor is limited in size for active noise control, virtual acoustic sensors were developed to shift the zone of quiet to a desired location that is remote from the physical error sensor. A number of virtual sensing methods have been developed to project the zone of quiet away from the physical microphone to a virtual location including *the virtual microphone arrangement* (Elliott and David 1992), *the remote microphone technique* (Roure and Albarrazin 1999), *the forward difference prediction technique* (Cazzolato 1999), *the adaptive LMS virtual microphone technique* (Cazzolato 2002), *the Kalman filtering virtual sensing method* (Petersen et al. 2008) and *the Stochastically Optimal Tonal Diffuse Field (SOTDF) virtual sensing method* (Moreau et al. 2009).

Spatially fixed virtual sensing methods

The virtual microphone arrangement (Elliott and David 1992) projects the zone of quiet away from the physical microphone using the assumption of equal primary sound pressure at the physical and virtual locations. A preliminary identification stage is required in this virtual sensing method in which models of the transfer functions between the secondary source and microphones located at the physical and virtual locations are estimated. These secondary transfer functions, along with the assumption of equal sound pressure at the physical and virtual locations, are used to obtain an estimate of the error signal at the virtual location given the physical error signal. The remote microphone technique (Roure and Albarrazin 1999) is an extension to the virtual microphone arrangement that uses an additional filter to compute an estimate of the primary pressure at the virtual location using the primary pressure at the physical microphone location.

The forward difference prediction technique (Cazzolato 1999) fits a polynomial to the signals at a number of microphones in an array. The pressure at the virtual location is estimated by extrapolating this polynomial to the virtual location. The forward difference prediction technique does not require a preliminary identification stage nor FIR filters or similar to model the complex transfer functions between the error sensors and the sources. Furthermore, this is a fixed gain prediction technique that can accommodate to physical changes that may alter the complex transfer functions between the error sensors and the sources.

The adaptive LMS virtual microphone technique (Cazzolato 2002) employs the LMS algorithm to adapt the weights of physical microphones in an array so that the weighted sum of these signals minimises the mean square difference between the predicted pressure and that measured by a microphone placed at the virtual location. Once the weights have converged they are fixed and the microphone at the virtual location is removed.

The Kalman filtering virtual sensing method (Petersen et al. 2008) uses Kalman filtering theory to obtain an optimal estimate of the error signal at the virtual location. In this virtual sensing method, the active noise control system is modelled as a state-space system whose outputs are the physical and virtual error signals. Estimates of the plant states are first calculated using the physical error signals and then estimates of the virtual error signals are calculated using the estimated plant states.

The SOTDF virtual sensing method (Moreau et al. 2009) generates stochastically optimal virtual microphones specifically for use in diffuse sound fields using diffuse field theory. Like the forward difference prediction technique, this virtual sensing method does not require a preliminary identification stage nor models of the complex transfer functions between the error sensors and the sources. The SOTDF virtual sensing method is a fixed scalar weighting method requiring only sensor position information and as such can adapt to the physical changes that may alter the complex transfer functions between the error sensors and the sources.

Moving virtual sensing methods

Even though the sound is significantly attenuated at the virtual location with these virtual sensing algorithms, the spatial extent of the zone of quiet is still impractically small. A human observer with a virtual sensor located at their ear would experience dramatic changes in sound pressure level with only minor head movements. Subsequently, a number of moving virtual sensing methods that create a zone of quiet capable of tracking a one-dimensional trajectory in a one-dimensional sound field were developed including the remote moving microphone technique (Petersen et al. 2006), the adaptive LMS moving virtual microphone technique (Petersen et al. 2007) and the Kalman filtering moving virtual sensing method (Petersen 2007). These moving virtual sensing methods employ the remote microphone technique, the adaptive LMS virtual microphone technique and the Kalman filtering virtual sensing method respectively. The performance of these moving virtual sensors has been investigated in an acoustic duct, and experimental results demonstrated that minimising the moving virtual error signal achieved greater attenuation at the moving virtual location than minimising the error signal at either a fixed physical microphone or a fixed virtual microphone. Recently, Moreau et al. (2008a, 2008b) investigated the performance of the remote moving microphone technique in generating a virtual microphone that tracks the ear of a rotating artificial head in a three-dimensional sound field. Again, experimental results confirmed that moving virtual sensors provide improved attenuation at the moving virtual location compared to fixed virtual or fixed physical sensors.

Current work

This paper reports development of the Stochastically Optimal Tonal Diffuse Field (SOTDF) moving virtual sensing method. This moving virtual sensing algorithm generates a stochastically optimal virtual microphone capable of tracking a three-dimensional trajectory in a three-dimensional sound field. It employs the SOTDF virtual sensing method to obtain an estimate of the error signal at the moving virtual location. As diffuse sound fields are described statistically, this moving virtual sensing method characterises the statistically optimal relationship between a physical microphone and a moving virtual microphone in a diffuse sound field. The results achieved with the SOTDF moving virtual sensing method represent the average control performance at a number of different sensor locations within the sound field. Of considerable significance is that the SOTDF moving virtual sensing method does not require a preliminary identification stage nor models of the complex transfer functions between the error sensors and the sources. The performance of an active noise control system in generating a zone of quiet at a stochastically optimal virtual microphone located at the ear of a rotating artificial head has been investigated in real-time experiments in a modally dense sound field and the experimental results are presented here.

It should be noted that the SOTDF moving virtual sensing method employs the SOTDF virtual sensing method which has been developed specifically for use in pure tone diffuse sound fields. The performance of SOTDF virtual sensors has been numerically and experimentally investigated in a pure tone diffuse sound field (Moreau et al. 2009) and the results indicate that this virtual sensing method performs as predicted by diffuse field theory. In many real world applications however, its is likely that the sound field is not perfectly diffuse. In this paper, the SOTDF moving virtual sensing method is investigated in a modally dense sound field and therefore the experimental results presented here demonstrate the performance of SOTDF virtual sensors in a sound field that is not perfectly diffuse.

THEORY

The SOTDF moving virtual sensing method generates a stochastically optimal moving virtual microphone that tracks a three-dimensional trajectory in a three-dimensional sound field. To create a zone of quiet at the moving virtual microphone, the active noise control system must minimise the virtual error signal, $\hat{p}(\mathbf{x}_v(n))$, at the moving virtual location, $\mathbf{x}_v(n)$, estimated using the SOTDF moving virtual sensing method. The SOTDF moving virtual sensing method uses the SOTDF virtual sensing method (Moreau et al. 2009) to obtain an estimate of the moving virtual error signal. An overview of the SOTDF moving virtual sensing method is provided as follows. Full details of the SOTDF virtual sensing algorithm used in this moving virtual sensing method can be found in Moreau et al. (2009).

The SOTDF virtual sensing method calculates a stochastically optimal estimate of the virtual error signal at a spatially fixed virtual location using diffuse field theory. In derivation of this algorithm, the primary acoustic field is considered diffuse and the sound field contributions due to each of the secondary sources are modelled as uncorrelated single diffuse acoustic fields. The pressure at a point $\mathbf{x}$ in a single diffuse acoustic field is given by $p(\mathbf{x})$ and the x-axis component of pressure gradient at a point $\mathbf{x}$ in this field is given by $g_i(\mathbf{x})$.

For a displacement vector, $\mathbf{r} = r_x\mathbf{i} + r_y\mathbf{j} + r_z\mathbf{k}$, the following functions are defined:

$$A(\mathbf{r}) = \text{sinc}(k|\mathbf{r}|), \tag{1}$$

$$B(\mathbf{r}) = \frac{\partial A(\mathbf{r})}{\partial r_x} = -k\left(\frac{\text{sinc}(k|\mathbf{r}|) - \cos(k|\mathbf{r}|)}{k|\mathbf{r}|}\right)\left(\frac{r_x}{|\mathbf{r}|}\right), \tag{2}$$

$$\begin{aligned} C(\mathbf{r}) &= \frac{\partial^2 A(\mathbf{r})}{\partial r_x^2} \\ &= -k^2\left[\text{sinc}(k|\mathbf{r}|)\left(\frac{r_x}{|\mathbf{r}|}\right)^2 + \right. \\ &\quad \left.\left(\frac{\text{sinc}(k|\mathbf{r}|) - \cos(k|\mathbf{r}|)}{(k|\mathbf{r}|)^2}\right)\left(1 - 3\left(\frac{r_x}{|\mathbf{r}|}\right)^2\right)\right]. \end{aligned} \tag{3}$$

The correlations between the pressures and pressure gradients at two different points $\mathbf{x}_j$ and $\mathbf{x}_k$ separated by $\mathbf{r}$ are given by (Elliott and Garcia-Bonito 1995)

$$\langle p(\mathbf{x}_j)p^\star(\mathbf{x}_k)\rangle = A(\mathbf{r})\,\langle|p|^2\rangle, \tag{4}$$

$$\langle p(\mathbf{x}_j)g^\star(\mathbf{x}_k)\rangle = -B(\mathbf{r})\,\langle|p|^2\rangle, \tag{5}$$

$$\langle g(\mathbf{x}_j)p^\star(\mathbf{x}_k)\rangle = B(\mathbf{r})\,\langle|p|^2\rangle, \tag{6}$$

$$\langle g(\mathbf{x}_j)g^\star(\mathbf{x}_k)\rangle = -C(\mathbf{r})\,\langle|p|^2\rangle, \tag{7}$$

where $\langle\cdot\rangle$ denotes spatial averaging and $\star$ indicates complex conjugation. In the case that $\mathbf{x}_j$ and $\mathbf{x}_k$ are the same point, the limits of $A(\mathbf{r})$, $B(\mathbf{r})$ and $C(\mathbf{r})$ as $\mathbf{r} \to 0$ must be taken.

If there are m sensors in the field, then define $\mathbf{p}$ as an $m \times 1$ matrix whose elements are the relevant pressures or pressure gradients measured by the sensors. The pressure and the pressure

gradient at any point in the diffuse sound field can be expressed as the weighted sum of the m components, each of which are perfectly correlated with a corresponding element of $\mathbf{p}_i$, and a component which is perfectly uncorrelated with each of the elements. Therefore, for each position $\mathbf{x}$, the pressure $p(\mathbf{x})$ can be written as

$$p(\mathbf{x}) = \mathbf{H}_p(\mathbf{x})\mathbf{p} + p_u(\mathbf{x}), \tag{8}$$

where $\mathbf{H}_p(\mathbf{x})$ is a matrix of real scalar weights which are a function of the position $\mathbf{x}$ only and $p_u(\mathbf{x})$ is perfectly uncorrelated with the elements of $\mathbf{p}$. It can be shown, by postmultiplying the expression for $p(\mathbf{x})$ by $\mathbf{p}^{\mathrm{H}}$ and spatially averaging, that

$$\mathbf{H}_p(\mathbf{x}) = \mathbf{L}_p(\mathbf{x})\mathbf{M}^{-1}, \tag{9}$$

where

$$\mathbf{L}_p(\mathbf{x}) = \frac{\langle p(\mathbf{x})\mathbf{p}^{\mathrm{H}}\rangle}{\langle |p|^2\rangle}, \tag{10}$$

$$\mathbf{M} = \frac{\langle \mathbf{p}\mathbf{p}^{\mathrm{H}}\rangle}{\langle |p|^2\rangle}. \tag{11}$$

Matrices $\mathbf{L}_p(\mathbf{x})$ and $\mathbf{M}$ can be found using Eqs. (1) - (7). The aim here is to estimate the pressure at a virtual location. In order to do this, $p(\mathbf{x})$ must be estimated from the known quantities in $\mathbf{p}$. The pressure at any point $\mathbf{x}$ is given by Eq. (8). If only the measured quantities in $\mathbf{p}$ are known, then the best estimate of $p_u(\mathbf{x})$ is zero since it is perfectly uncorrelated with the measured signals. Therefore the best estimate of the pressure at a spatially fixed location, $\mathbf{x}$, is given by

$$\hat{p}(\mathbf{x}) = \mathbf{H}_p(\mathbf{x})\mathbf{p}. \tag{12}$$

It follows that the best estimate of the pressure at the moving virtual location, $\mathbf{x}_v(n)$, is given by

$$\hat{p}(\mathbf{x}_v(n)) = \mathbf{H}_p(\mathbf{x}_v(n))\mathbf{p}. \tag{13}$$

In this paper, the pressure at the moving virtual location is estimated using

1. The measured pressure and pressure gradient at a point.
2. The measured pressures at two points.
3. The measured pressures at three points.

In each of these three sensing strategies, the pressure at the moving virtual location is estimated using Eq. (13). This requires matrix $\mathbf{p}$ whose elements are the relevant pressures and pressure gradients measured by the physical sensors and calculation of the weight matrix $\mathbf{H}_p(\mathbf{x})$ using $\mathbf{L}_p(\mathbf{x})$ and $\mathbf{M}$ defined in Eqs. (10) and (11).

To create a zone of quiet at the moving virtual location, $\mathbf{x}_v(n)$, the SOTDF moving virtual sensing algorithm is combined with the filtered-x LMS algorithm (Nelson and Elliott 1992). The filtered-x LMS algorithm is used to generate the control signal to the secondary loudspeaker using the estimated moving virtual error signal, $\hat{p}(\mathbf{x}_v(n))$. Details of the filtered-x LMS algorithm may be found in Nelson and Elliott (1992), Kuo and Morgan (1996) and Elliott (2001).

EXPERIMENTAL METHOD

The performance of an active noise control system in generating a moving zone of quiet at one of the ears of a rotating artificial head has been investigated in real-time experiments conducted in a three-dimensional cavity. The cavity has dimensions of 1 m $\times$ 0.8 m $\times$ 0.89 m and a volume of 0.712 m^3. A HEAD acoustics HMS III.0 Artificial Head, mounted on a turntable to simulate head rotation, is located in the centre of the cavity, as shown in Fig. 1. The artificial head has overall dimensions of 0.465 m $\times$ 0.4 m $\times$ 0.18 m to approximate the size of a human head. The turntable is position controlled to generate 90° head rotations from $-45°$ to $+45°$ which is typical of the complete head rotations capable of a seated observer. The desired trajectory of the artificial head and of the virtual microphone is a triangular waveform with peak amplitudes of $\pm 45°$. The expression of the triangular waveform governing the desired head rotations, in degrees, is given by

$$\theta_h(n) = \frac{180}{\pi}\arcsin\left(\sin\left(\frac{2\pi n}{t_v f_s}\right)\right), \tag{14}$$

where n is the time sample, t_v is the period of the head motion and $f_s = 2.5$ kHz the sampling frequency.

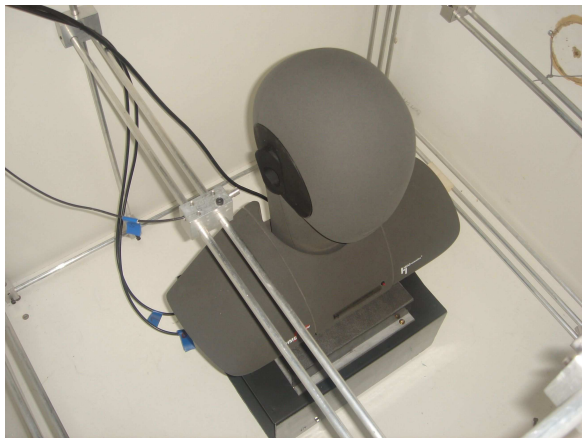

Figure 1: The HEAD acoustics HMS III.0 Artificial Head mounted on a turntable and located in the centre of the cavity. The fixed frame supports the physical microphones.

The SOTDF moving virtual sensing method is implemented in three forms; using the measured pressure and pressure gradient at a point, the measured pressures at two points and the measured pressures at three points. Using the measured pressure and pressure gradient to estimate the moving virtual error signal requires simultaneous measurement of the pressure and pressure gradient at the same location and this was done using the two microphone technique (Fahy 1995) in real-time experiments. In the two-microphone technique, the pressure is estimated midway between two physical microphones and the pressure gradient is calculated using a finite difference approximation. When using the measured pressure and pressure gradient at a point or the pressures at two points to estimate the moving virtual error signal, the two physical microphones were arranged in linear parallel formation, as shown in Fig. 2. In this case, the centre point between the two physical microphones was 4 cm from the ear when the artificial head was positioned at $\theta_h = 0°$ and the physical microphone spacing was 2 cm. When using the measured pressures at three points to estimate the moving virtual error signal, the three physical microphones were arranged in triangular formation as is shown in Fig. 3. In this case, the three physical microphones were located on the corners of an isosceles triangle with equal angles of 30°. An additional electret microphone was also located at the ear of the artificial head to measure the performance at the virtual microphone position.

Two 4" loudspeakers were located in the opposite corners of the cavity, one to generate the tonal primary sound field and the other to act as the control source. The performance of the active noise control system at the moving virtual location was investigated at the excitation frequency of 525 Hz which corresponds to the 33rd acoustic resonance. At this frequency, the modal

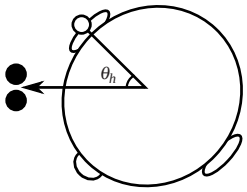

(a) $\theta_h = -45°$.

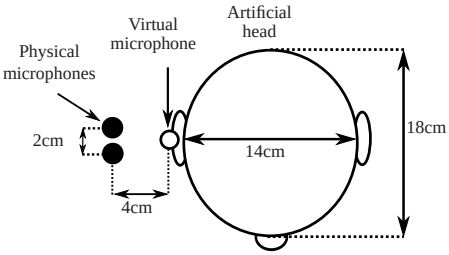

(b) $\theta_h = 0°$.

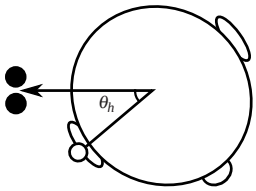

(c) $\theta_h = 45°$.

Figure 2: The physical arrangement of the artificial head and the physical and virtual microphones when using the measured pressure and pressure gradient at a point or the measured pressures at two points to estimate the moving virtual error signal. The physical microphones are indicated by solid circle markers and the virtual microphone is indicated by an open circle marker.

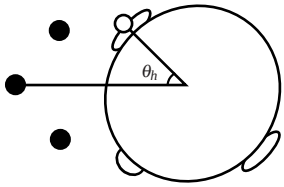

(a) $\theta_h = -45°$.

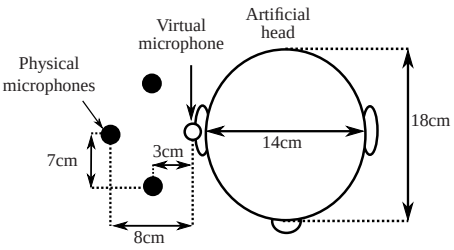

(b) $\theta_h = 0°$.

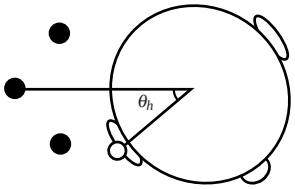

(c) $\theta_h = 45°$.

Figure 3: The physical arrangement of the artificial head and the physical and virtual microphones when using the measured pressures at three points to estimate the moving virtual error signal. The physical microphones are indicated by solid circle markers and the virtual microphone is indicated by an open circle marker.

overlap is $M = 4$ illustrating that the sound field is modally dense, as a modal overlap of $M = 3$ defines the boundary between low and high modal density (Nelson and Elliott 1992). The performance of the moving virtual sensing algorithm was also investigated off resonance, at an excitation frequency of 510 Hz. An excitation frequency of 510 Hz lies between the 31st and 32nd resonant frequency. For both excitation frequencies of 525 Hz and 510 Hz, the performance at the moving virtual location was measured for two different periods of 90° head rotation; $t_v = 5$ s and $t_v = 10$ s.

The host-target software program XPC TARGET was used to implement the SOTDF moving virtual sensing method and the filtered-x LMS algorithm in real-time. The filtered-x LMS algorithm was implemented using a two coefficient control filter.

EXPERIMENTAL RESULTS

The time average and standard deviation of the attenuation achieved at the moving virtual location with the three different physical sensor configurations at the 525 Hz resonance is given in Table 1. Results are given for active noise control at the moving virtual microphone, a fixed virtual microphone located at the ear of the rotating artificial head when $\theta_h = 0°$ and the fixed physical microphone located 4 cm from the ear when $\theta_h = 0°$. The results of real-time experimental control have been generated by averaging the results over a number of data sets. This is because this moving virtual sensing method gives a stochastically optimal estimate of the virtual error signal at the moving virtual location. To obtain a number of data sets to provide the spatial average, the rotating artificial head and the sensors were located at ten different positions within the cavity while ensuring the relative arrangement of the sensors and the rotating artificial head remained constant. The results in Table 1 have been generated by averaging the results of active noise control at the 10 different locations.

For all three physical sensor configurations and both periods of head rotation, Table 1 reveals that minimising the moving virtual error signal achieves the greatest attenuation at the moving virtual location. Comparing the time-averaged attenuations achieved with the three different physical sensor configurations in Table 1 demonstrates that using the measured pressures at three points to estimate the moving virtual error signal generates the best control performance at the ear of the rotating artificial head. Such a result is to be expected given that the three-dimensional configuration of three physical microphones in triangular formation should more accurately model the three-dimensional sound field than the one-dimensional physical sensor configuration of two physical microphones in linear formation. An additional 1.5 dB of attenuation is achieved when using the measured pressures at three points to estimate the moving virtual error signal compared to using the other physical sensor configurations. The standard deviation of the attenuation is also significantly smaller when using the measured pressures at three points to estimate the moving virtual error signal, indicating a smaller variation in sound pressure level with head movement. Table 1 also indicates that minimising the moving virtual error signal estimated using the measured pressures at three points provides up to an additional 6.3 dB of attenuation compared to minimising the fixed virtual error signal. Active noise control at the moving virtual microphone achieves up to an additional 15.6 dB of attenuation at the moving virtual location compared to active noise control at the fixed physical microphone.

Table 1 also shows a decrease in the attenuation and an increase in the standard deviation with a decrease in the period of head rotation. Such a result is to be expected because it takes a finite time for the controlled sound field to stabilise, so once the period of head rotation nears the reverberation time of the cavity, the control performance is compromised.

Figs. 4 and 5 show the attenuation achieved at the moving virtual location at 525 Hz and 510 Hz respectively when using the measured pressures at three points to estimate the virtual error signals. Average control profiles are shown for active noise control at the moving virtual microphone, a fixed virtual microphone located at the ear of the rotating artificial head when $\theta_h = 0°$ and the fixed physical microphone located 4 cm from the ear when $\theta_h = 0°$. The average control performance at the ear of the rotating artificial head is shown for the period of head rotation of $t_v = 10$ s in part (a) of Figs. 4 and 5 and $t_v = 5$ s in part (b) of Figs. 4 and 5. Part (c) of Figs. 4 and 5 shows the desired trajectory of the artificial head and of the moving virtual microphone, in degrees, compared to the actual controlled head position. The actual controlled head position is used in the moving virtual sensing algorithm to calculate the physical sensor weights. The transient behaviour seen in Figs. 4 and 5 at time $t/t_v = 0$ s for both $t_v = 5$ s and $t_v = 10$ s, is caused by the controller initialising.

The control profiles in Figs. 4 and 5 demonstrate that minimising the moving virtual error signal estimated using the SOTDF moving virtual sensing method generates the best control performance at the ear of the rotating artificial head. At the 525 Hz resonance, Fig. 4 (a) shows that when $t_v = 10$ s, active noise control at the moving virtual microphone achieves an attenuation of between 20 dB and 28 dB at the ear of the artificial head. Minimising the fixed virtual error signal generates a maximum attenuation of 24 dB at the ear of the artificial head when $\theta_h = 0°$ and a minimum attenuation of 12 dB when $\theta_h = 45°$. In comparison, active noise control at the physical microphone achieves an attenuation at the ear of the rotating artificial head of between only 1 dB and 20 dB. When the period of head rotation is reduced to $t_v = 5$ s, Fig. 4 (b) shows that minimising the moving virtual error signal results in an attenuation of between 20 dB and 27 dB being achieved at the ear of the artificial head. This is an improvement in control performance compared to active noise control at either the fixed virtual or physical microphone where the attenuation levels again fall to 12 dB and 1 dB respectively when $\theta_h = 45°$.

Comparing Figs. 4 and 5 shows that reduced control performance is achieved off resonance. This is because a number of modes contribute to the cavity response when the primary noise disturbance is off resonance. When $t_v = 10$ s, minimising the moving virtual error signal off resonance achieves between 14 dB and 28 dB of attenuation at the ear of the artificial head as shown in Fig. 5 (a). Minimising the fixed virtual error signal achieves a maximum attenuation of 19 dB at the ear of the artificial head when $\theta_h = 0°$ and a minimum attenuation of 9 dB when $\theta_h = 45°$. Active noise control at the physical microphone achieves 19 dB of attenuation at the ear of the artificial head when $\theta_h = 0°$ and only 1 dB of attenuation when $\theta_h = 45°$. When the period of head rotation is $t_v = 5$ s, Fig. 5 (b) shows that minimising the moving virtual error signal results in an attenuation of between 16 dB and 25 dB being achieved at the ear of the moving virtual location. This is an improvement in control performance compared to active noise control at either the fixed virtual or physical microphone where attenuation levels again fall to 10 dB and 1 dB respectively when $\theta_h = 45°$.

Table 2 gives the time average and standard deviation of the attenuation achieved at the moving virtual location for off resonance excitation when the virtual error signals are estimated using the measured pressures at three points. Tabulated results are given for active noise control at the moving virtual microphone, a fixed virtual microphone located at the ear of the arti-

Table 1: Time average and standard deviation (in parenthesis) of the attenuation in dB achieved at the moving virtual location at the 525 Hz resonance with the SOTDF moving virtual sensing method.

	Using the measured pressure and pressure gradient at a point			**Using the measured pressures at two points**			**Using the measured pressures at three points**		
$t_v(s)$	Moving virtual mic	Fixed virtual mic	Fixed physical mic	Moving virtual mic	Fixed virtual mic	Fixed physical mic	Moving virtual mic	Fixed virtual mic	Fixed physical mic
10	22.4(4.2)	18.0(4.1)	9.1(5.3)	22.4(4.5)	17.1(4.9)	9.2(4.3)	23.9(2.8)	17.6(3.4)	9.1(4.3)
5	21.4(4.3)	16.5(4.2)	7.1(4.8)	21.3(4.6)	16.1(4.7)	7.4(4.8)	22.7(3.2)	17.2(3.5)	7.1(4.8)

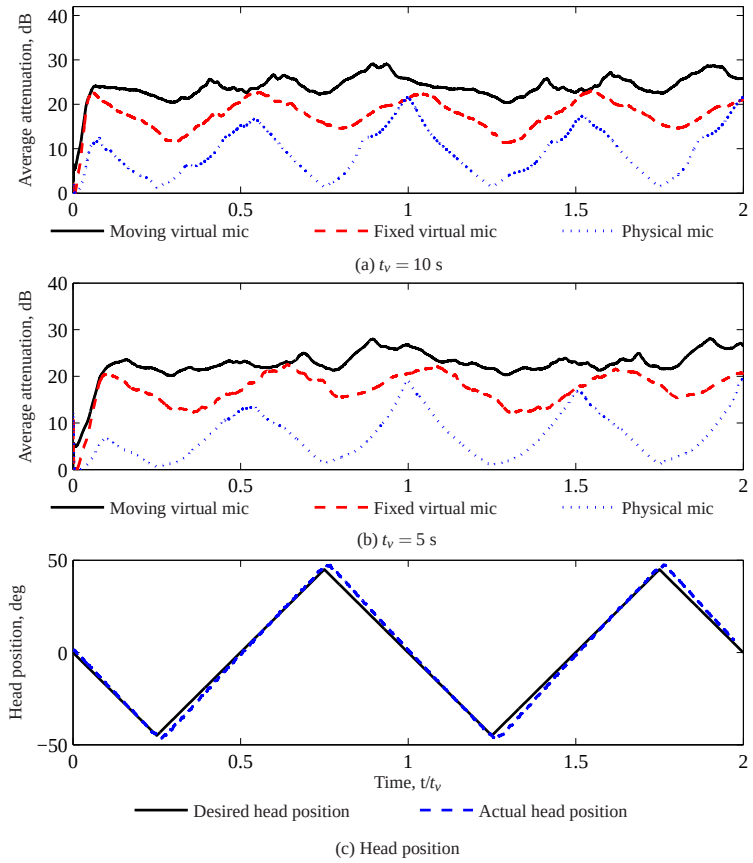

(a) $t_v = 10$ s

(b) $t_v = 5$ s

(c) Head position

Figure 4: The average tonal attenuation achieved at the moving virtual location at the 525 Hz resonance with the SOTDF moving virtual sensing method using the measured pressures at three points (physical sensor arrangement shown in Fig. 3). Control profiles are shown for active noise control at the moving virtual microphone, a virtual microphone spatially fixed at $\theta_h = 0^\circ$ and the physical microphone, for a period of rotation (a) $t_v = 10$ s; (b) $t_v = 5$ s; and (c) head position.

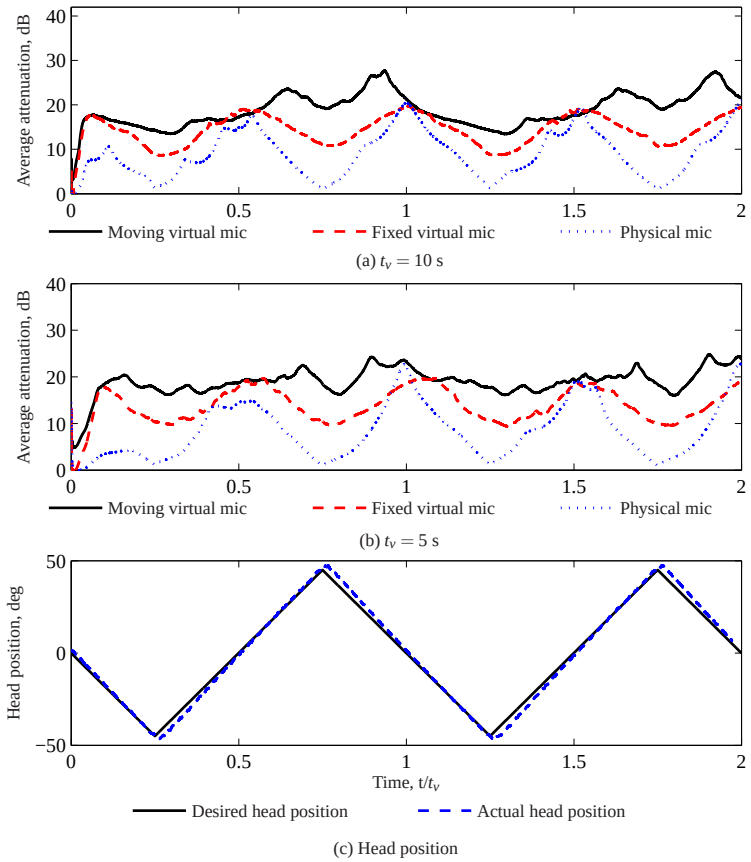

(a) $t_v = 10$ s

(b) $t_v = 5$ s

(c) Head position

Figure 5: The average tonal attenuation achieved at the moving virtual location off resonance at 510 Hz with the SOTDF moving virtual sensing method using the measured pressures at three points (physical sensor arrangement shown in Fig. 3). Control profiles are shown for active noise control at the moving virtual microphone, a virtual microphone spatially fixed at $\theta_h = 0^\circ$ and the physical microphone, for a period of rotation (a) $t_v = 10$ s; (b) $t_v = 5$ s; and (c) head position.

Table 2: Time average and standard deviation (in parenthesis) of the attenuation in dB achieved at the moving virtual location on and off resonance with the SOTDF moving virtual sensing method when the virtual quantities are estimated using the measured pressures at three points.

	525 Hz			**510 Hz**		
$t_v(s)$	Moving virtual mic	Fixed virtual mic	Fixed physical mic	Moving virtual mic	Fixed virtual mic	Fixed physical mic
10	23.9(2.8)	17.6(3.4)	9.1(4.3)	21.5(3.8)	15.7(4.1)	8.9(5.2)
5	22.7(3.2)	17.2(3.5)	7.1(4.8)	18.9(3.9)	17.1(4.2)	8.3(5.7)

ficial head when $\theta_h = 0^\circ$ and the fixed physical microphone. Table 2 reveals that for active noise control of off resonance excitation at the moving virtual microphone provides up to an additional 5.8 dB of attenuation at the moving virtual location compared to active noise control at the fixed virtual microphone. Minimising the moving virtual error signal achieves up to an additional 12.6 dB of attenuation at the moving virtual location compared to minimising the physical error signal.

Comparing the average attenuations achieved at the two excitation frequencies in Table 2 demonstrates that reduced control performance is achieved off resonance. Table 2 also confirms that as the period of head rotation decreases, the average attenuation achieved at the moving virtual location decreases and the standard deviation increases.

The experimental results presented in Tables 1 and 2 and Figs. 4 and 5 show the performance of the SOTDF moving virtual sensing method in a sound field that is not perfectly diffuse. Active noise control at the moving virtual sensors provides improved attenuation at the ear of the rotating artificial head compared to minimising either the fixed virtual error signal or fixed physical error signal in a modally dense sound field. This demonstrates that stochastically optimal moving and fixed virtual sensors are suitable for use in a sound field that is not perfectly diffuse.

CONCLUSION

By considering the pressure to have components perfectly spatially correlated and perfectly uncorrelated with the measured quantities in a diffuse sound field, a prediction algorithm for stochastically optimal moving virtual sensors has been derived. This moving virtual sensing algorithm generates a stochastically optimal virtual microphone capable of tracking a three-dimensional trajectory in a three-dimensional sound field.

The performance of an active noise control system in generating a zone of quiet at a virtual microphone located at a single ear of a rotating artificial head has been experimentally investigated in a modally dense sound field. Experimental results demonstrate that greater attenuation can be achieved at the moving virtual location when a stochastically optimal moving virtual sensor is employed compared to a stochastically optimal fixed virtual sensor or a fixed physical sensor. Experimental results also demonstrated that SOTDF moving and fixed virtual sensors are suitable for use in a sound field that is not perfectly diffuse.

It is worth noting that while greater control can be achieved at the moving virtual location with the deterministic remote moving microphone technique, the SOTDF moving virtual sensing method is much simpler to implement as it is a fixed weighting technique requiring only sensor position information. This also means that unlike the remote moving microphone technique, the SOTDF moving virtual sensing method is robust to changes in the sound field that may alter the transfer functions between the error sensors and the sources.

REFERENCES

B.S. Cazzolato. *Sensing systems for active control of sound transmission into cavities*. PhD thesis, Department of Mechanical Engineering, The University of Adelaide, SA, 1999.

B.S. Cazzolato. An adaptive LMS virtual microphone. In *Proceedings of Active 2002, ISVR*, pages 105–116, Southampton, UK, 2002.

S.J. Elliott. *Signal Processing for Active Control*. Academic Press, 2001.

S.J. Elliott and A. David. A virtual microphone arrangement for local active sound control. In *Proceedings of the 1st International Conference on Motion and Vibration Control*, pages 1027–1031, Yokohama, 1992.

S.J. Elliott and J. Garcia-Bonito. Active cancellation of pressure and pressure gradient in a diffuse sound field. *Journal of Sound and Vibration*, 186(4):696–704, 1995.

S.J. Elliott, P. Joseph, A.J. Bullmore, and P.A. Nelson. Active cancellation at a point in a pure tone diffuse sound field. *Journal of Sound and Vibration*, 120(1):183–189, 1988.

F. Fahy. *Sound Intensity*. E&FN Spon, 2nd edition, 1995.

C.H. Hansen and S.D. Snyder. *Active control of noise and vibration*. E and FN Spon, 1997.

S.M. Kuo and D.R. Morgan. *Active Noise Control Systems, Algorithms and DSP Implementation*. John Wiley and Sons, Inc, 1996.

D.J. Moreau, B.S. Cazzolato, and A.C. Zander. Active noise control at a moving location in a modally dense three-dimensional sound field using virtual sensing. In *Proceedings of Acoustics 08*, Paris, 2008a.

D.J. Moreau, B.S. Cazzolato, and A.C. Zander. Active noise control at a moving virtual sensor in three dimensions. *Acoustics Australia*, 36(3):93–86, 2008b.

D.J. Moreau, J. Ghan, B.S. Cazzolato, and A.C. Zander. Active noise control in a pure tone diffuse sound field using virtual sensing. *Journal of the Acoustical Society of America*, 125(6):3742–3755, 2009.

P.A. Nelson and S.J. Elliott. *Active Control of Sound*. Academic Press, 1st edition, 1992.

C.D. Petersen. *Optimal spatially fixed and moving virtual sensing algorithms for local active noise control*. PhD thesis, School of Mechanical Engineering, The University of Adelaide, 2007.

C.D. Petersen, B.S. Cazzolato, A.C. Zander, and C.H. Hansen. Active noise control at a moving location using virtual sensing. In *ICSV13: Proceedings of the 13th International Congress of Sound and Vibration*, Vienna, 2006.

C.D. Petersen, R. Fraanje, B.S. Cazzolato, A.C. Zander, and C.H. Hansen. A Kalman filter approach to virtual sensing for active noise control. *Mechanical Systems and Signal Processing*, 22(2):490–508, 2008.

C.D. Petersen, A.C. Zander, B.S. Cazzolato, and C.H. Hansen. A moving zone of quiet for narrowband noise in a one-dimensional duct using virtual sensing. *Journal of the Acoustical Society of America*, 121(3):1459–1470, 2007.

A. Roure and A. Albarrazin. The remote microphone technique for active noise control. In *Proceedings of Active 99*, pages 1233–1244, 1999.